Durability of Carbon Nanofiber (CNF) & Carbon Nanotube (CNT) as Catalyst Support for Proton Exchange Membrane Fuel Cells

Andersen, Shuang Ma; Borghei, Maryam ; Lund, Peter ; Elina, Yli-Rantala ; Pasanen, Antti ; Kauppinen, Esko ; Ruiz, Virginia ; Kauranen, Pertti ; Skou, Eivind Morten

Published in:
Solid State Ionics

DOI:
10.1016/j.ssi.2012.11.020

Publication date:
2013

Document Version
Final published version

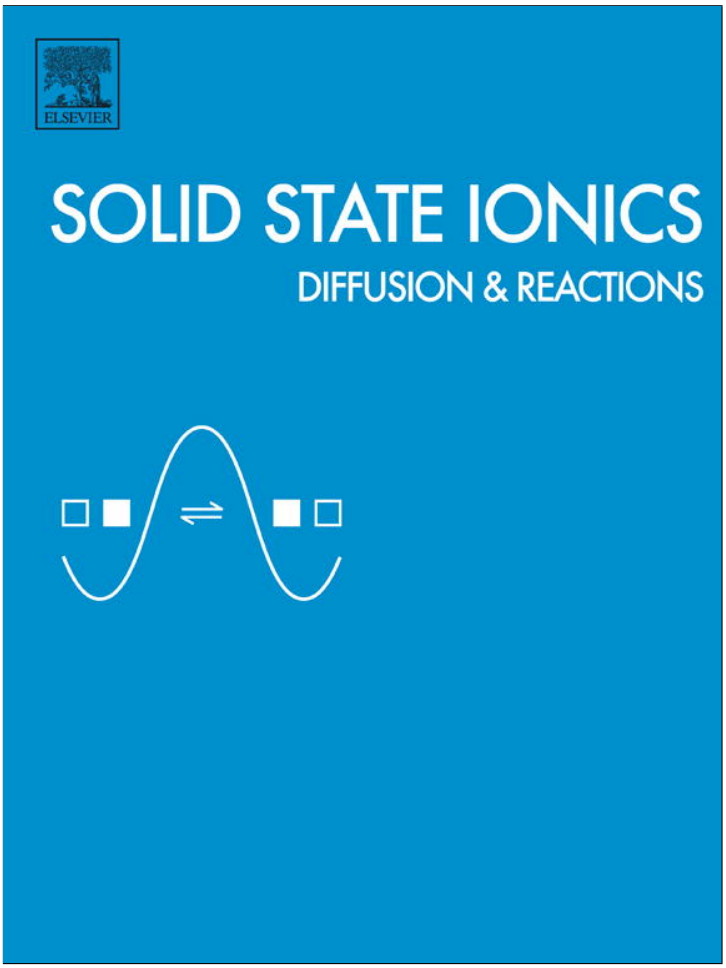

(This is a sample cover image for this issue. The actual cover is not yet available at this time.)

Solid State Ionics 231 (2013) 94–101

Contents lists available at SciVerse ScienceDirect

Solid State Ionics

journal homepage: www.elsevier.com/locate/ssi

Durability of carbon nanofiber (CNF) & carbon nanotube (CNT) as catalyst support for Proton Exchange Membrane Fuel Cells

Shuang Ma Andersen [a,*], Maryam Borghei [b], Peter Lund [c], Yli-Rantala Elina [d], Antti Pasanen [d], Esko Kauppinen [b], Virginia Ruiz [e], Pertti Kauranen [d], Eivind M. Skou [a]

[a] Institute of Chemical Engineering, Biotechnology and Environmental Technology, University of Southern Denmark, Denmark
[b] NanoMaterials Group, Department of Applied Physics, Aalto University, Finland
[c] IRD Fuel Cells A/S, Svedberg, Denmark
[d] VTT Technical Research Centre of Finland, Tampere, Finland
[e] CIDETEC-IK4, Centre for Electrochemical Technologies, Paseo Miramón 196, E-20009 Donostia-San Sebastián, Spain

ARTICLE INFO

Article history:
Received 29 May 2012
Received in revised form 1 November 2012
Accepted 25 November 2012
Available online xxxx

Keywords:
CNF
CNT
Catalyst support
PEM fuel cells
Durability

ABSTRACT

Durability issues have recently been given much attention in Proton Exchange Membrane Fuel Cell (PEMFC) research. It gives fundamental definition for cell life time, capital cost, system stability and technique reliability. Loss of catalyst surface area due to corrosion of supporting material (normally carbon black) is one of the essential degradation mechanisms during cell operation. In this work, durability of carbon nanofibers (CNF) & carbon nanotubes (CNT) as alternative platinum catalyst supports for Proton Exchange Membrane Fuel Cells (PEMFCs) was assessed. Platinized CNF and CNT using a standard polyol method were prepared and fabricated as cathodes of Membrane Electrode Assemblies (MEA) for PEMFC. Both the catalysts as such and the MEAs made out of them were evaluated regarding to thermal and electrochemical stabilities using traditional carbon black (Vulcan XC72) as a reference. Thermal gravimetric analysis (TGA), cyclic voltammetry (CV), polarization curve and impedance spectroscopy were applied on the samples under accelerated stress conditions. The carbon nano-materials demonstrated better stability as a support for nano-sized platinum catalyst under PEMFC related operating conditions. Due to different morphology of the nano carbons compared to Vulcan XC 72 the electrode structures may still need optimization to improve the overall cell performance.

1. Introduction

Interest on carbon nano-materials can be traced back to more than two decades ago. Carbon nanofiber (CNF) and carbon nanotube (CNT) are receiving more and more attention since then due to their impressive thermal and electric properties in various areas [1], especially their huge potentials in fuel cell developments [2–5] and hydrogen storage [6,7] as demonstrated during the last 10 years.

Fuel cells (FC) bear the merits of high efficiency, renewability and low pollution. Among various types of FC, Proton Exchange Membrane Fuel Cell (PEMFC) is believed to be one of the most promising energy providers in the near future for terrestrial applications, military, as well as in stationary and portable power sources [8]. In order to achieve high catalytic surface area and reduce cost of PEMFC electrodes, nano-sized catalysts are normally supported on carbon. To enhance protonic conductivity, Nafion ionomer is often impregnated in the electrode structure. The region where electronic phase, protonic phase and gas phase meet is the so called three-phase-boundary (TPB), where electrochemical reactions take place.

In addition to reducing capital cost and improving electrode reaction efficiency, material durability is one of the key issues in the advancement of PEM fuel cell technology. Among numerous chemical, mechanical and thermal degradation challenges [9,10], loss of noble metal catalyst and consequent decline of cell performance due to instability of the supporting carbon (carbon corrosion) are two of the important failure modes for PEMFCs. Moreover, the degradation of carbon support and catalytic metals interacts with and exacerbates one another. On the one hand, oxidation of carbon is promoted by the platinum particles due to their catalytic effect; on the other hand, once the carbon supports are corroded, the catalysts lose their physical support, electrical contact, and balanced electrode structure, and consequently they have an overall decreased electrochemical active surface area [11,12].

Attractive candidates for more stable supports are modified carbon [13–15] nano-carbon [16–18], graphene nanosheets, titanium based supports [19,20] and nano-silicon carbide [21]. Here we will mainly focus on the potential of carbon nanofiber (CNF) and carbon nanotube (CNT) as platinum supports for low temperature PEMFCs.

Various techniques have been developed for platinizing catalyst supports. A comprehensive review has recently been published by Esmaeilifar et al. [22]. Each procedure has both advantages and disadvantages; among those, polyol process displays the possibility of high

* Corresponding author. Tel.: +45 6550 2579; fax: +45 6615 8780.
E-mail address: mashu@kbm.sdu.dk (S.M. Andersen).

0167-2738/$ – see front matter © 2012 Elsevier B.V. All rights reserved.
http://dx.doi.org/10.1016/j.ssi.2012.11.020

Table 1
List of carbon and carbon supported catalyst information.

No.	Name	Element content	Catalyst wt.%	Alloy ration	Carbon type	Catalyst or carbon diameter nm	Surface area m^2/g
1	CNF	C	0	–	CNF	150, length 10 μm	13
2	CNT	C	0	–	CNT	15, length 3 μm	270
3	Vulcan XC-72	C	0	–	Vulcan	~13	208.58
4	Ketjenblack	C	0	–	HSCB	~2	1421.24
5	CNF 20% Pt	Pt/C	20	–	CNF	2.79	10.49
6	CNT 20% Pt	Pt/C	20	–	CNT	3.10	90.44
7	Vulcan 20% Pt BASF	Pt/C	20	–	Vulcan	2.50	112.15
8	Hispec 9000	Pt/C	57.84	–	Vulcan	5.47	102.56
9	Hispec 9100	Pt/C	56.76	–	*	2.77	304.81
10	Hispec 10000	PtRu/C	59.72	1:1	Vulcan	2.90	114.4
11	Hispec 10100	PtRu/C	58.61	1:1	*	2.28	286.55
12	Blank	–	–	–	–	–	–

* Hispec 9100 and 10100 are using the same type of carbon support, however the detail is confidential.

platinum content and small particle size with uniform dispersion simultaneously, therefore, it is still one of the most popular techniques being studied and optimized [22,23].

In this work, thermal and electrochemical durability of carbon nanofiber and carbon nanotube supported platinum nano particles prepared by the polyol method was studied and compared to conventional commercial catalyst supports based on both ex-situ and in-situ experiments.

2. Experimental

2.1. Carbon nanomaterial supports and platinum deposition

Two types of carbon nano-materials synthesized by chemical vapor deposition and kindly supplied by Showa Denko (Japan), were used as catalyst supports, namely VGCF™ and VGCF-X™. Properties of the materials provided by the supplier are listed in Table 1. Deposition of ~20 wt.% Pt on CNFs was performed by the colloidal polyol method, according to a protocol reported elsewhere [24], which consists the reduction of the H_2PtCl_6 precursor to metallic Pt by ethylene glycol (EG) in alkaline media in the presence of the carbon support.

Morphology characterization of carbon nanomaterial supports and catalyst based on the support was carried out by Raman analysis using a Horiba LabRAM HR spectrometer equipped with a CCD camera and a 633 nm laser beam. Scanning Electron Microscopy (SEM) with a field emission gun using JEOL JSM-7500FA equipped with an energy dispersive X-ray spectrometer (EDXS) and Transmission Electron Microscopy (TEM) with a Tecnai 12 BioTwin with LaB6 gun at 120 kV.

2.2. Thermal stability of carbon

Thermal stability of the carbons was tested at 200 °C in a ventilated oven. Carbon or catalyst samples (Table 1) were packed individually in aluminum foil (quickpack, AL raffination®), the weight of which was proven to be stable during the treatment. The weights of the small packages were examined via a digital balance (Mettler AE260 DeltaRange®). The samples were pre-heated at 80 °C to eliminate adsorption of water. Since noble metal or noble metal alloy was proven to be stable under the condition [25], sample weight loss corresponds to carbon weight loss.

Table 2
Atomic adsorption spectroscopy program for Pt.

	Tem. (°C)	Ramp time (s)	Hold time (s)	Air flow (ml/min)
Drying	120	10	25	250
Pyrolysis	1400	10	20	250
Atomization	2700	0	10	0

2.3. Thermogravimetry — carbon thermal decomposition

Complete thermal decomposition of carbon under the influence of catalyst and/or ionomer was studied with thermogravimetry using Setaram TGA 92-12. In the measurement, about 3–4 mg powder was transferred to an aluminum oxide crucible for TG analysis. The initial and final temperature is 20 and 900 °C with a heating rate of 5 °C/min. The experiment was performed in a mixed argon and oxygen atmosphere of ratio 3:1, with a total pressure of one atmosphere.

The carbon/catalyst and Nafion ionomer mixture were prepared according to the following procedure. Suitable amounts of carbon/catalyst were weighted into 2 mL eppendorf tube, and then mixed with 1.5 mL of Nafion ionomer solution of 10^{-3} M. A thorough mixing of the solution and specimen powder was ensured by mechanical shaking (Holm & Halby, Eamund Bühler, KL-2) for 30 min and ultrasonicating in a water bath (Holm & Halby, Elma, TRANSSONIC TP 690) for 4 h for the supporting carbon and carbon supported catalyst, and 8 h for the metal or metal alloy catalysts. The maximum bath temperature was about 50 °C. Parafilm was used as a lid over the vessel to prevent evaporation. After mixing, the vessels were transferred to the centrifuge (Ole Dich Instrumentmaker APS, Microcentrifuge 157.MD). The samples were centrifuged for 1 h with 12,000 revolutions/min at 4 °C. The liquid phase (as much as possible) was taken out carefully by an auto pipette and kept for other usage. The remaining solid phase was kept in air at 40 °C for 12 h to evaporate the residual water. The final dry agglomerate was grinded in a jade mortar with a pestle to powder form.

2.4. Dispersion and coating of catalyst particles

The fabricated catalyst particles were ultrasonically dispersed in a water/alcohol suspension as solid polymer electrolyte Nafion® was used in a ratio of 40% (w/w). Control of dispersion was checked by measuring the particle size distribution using laser diffraction method (Malvern Mastersizer E). Typically dispersion was continued until the largest particles were below 10 μm, however, depending on the nature of the support material the dispersion was stopped if no progression in particle distribution was observed.

The suspension was coated onto a gas diffusion layer, Sigracet 35DC® (SGL Group) by ultrasonically spraying using a Prism 300/400 (USI, Ultrasonic Systems, Inc.). Typical platinum loading was 0.5 $mg \cdot cm^{-2}$. The MEA or half cell was constructed by laminating the coated gas diffusion layer onto Nafion® 212 [26].

2.5. Pt dissolution

A home developed Teflon cell was used for MEA catalyst degradation studies. The reference electrode was a chloride-free REF 601 Hg/Hg_2SO_4 (radiometer), which was placed in a separated chamber connected to the main cell through a Luggin capillary. The counter electrode (40 mm diameter) was a piece of clean carbon paper (GDL) with no extra

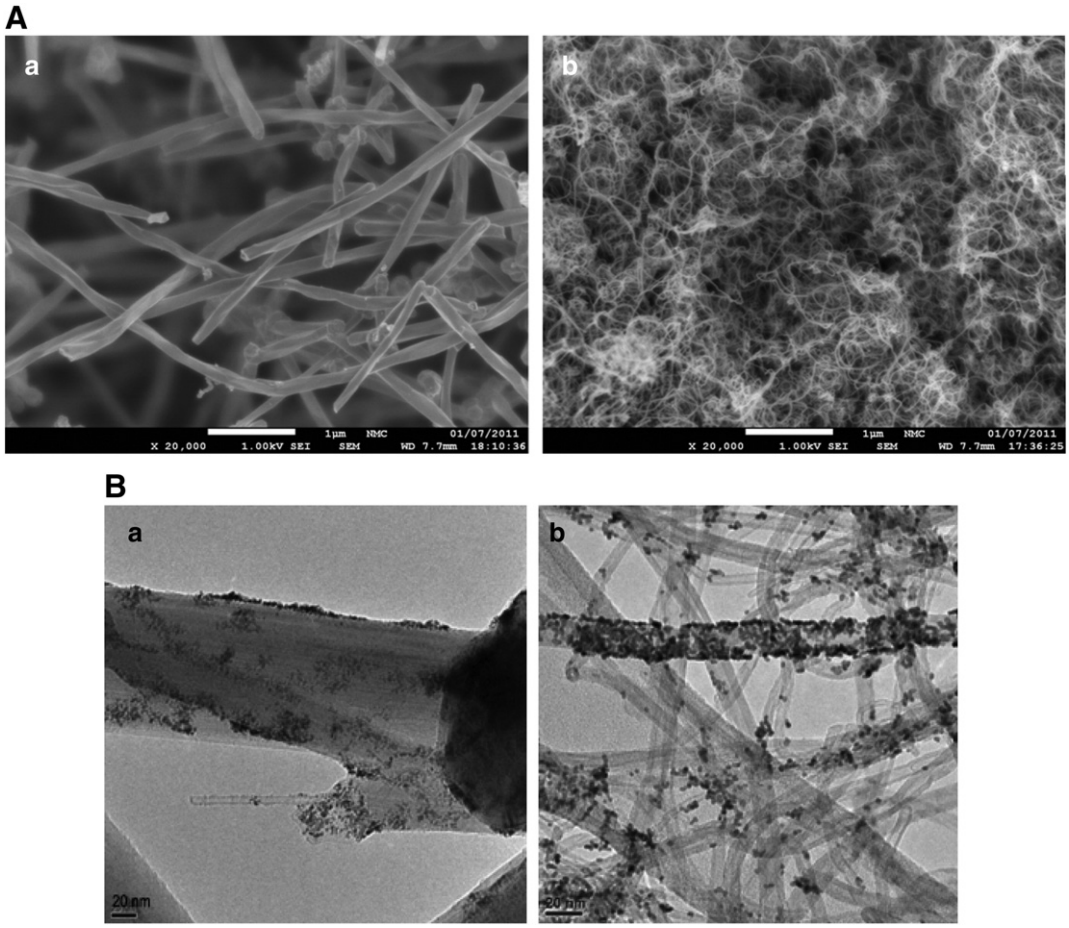

Fig. 1. (A) SEM images of the catalyst carbon supports: (a) CNF and (b) CNT. (B) TEM images of Pt deposited on: (a) CNF and (b) CNT.

additives. In order to avoid contamination, the GDL was discarded after each measurement. The working electrode was 12.4 mm in diameter. The total cell volume was about 20 mL. The liquid electrolyte was 1 M sulfuric acid. For dissolution studies, the potential sweep rate in cyclic voltammetry experiment was kept constant at 0.1 V/s; a 0.5 mL liquid sample was collected by a syringe at each potential step after 30 min potential cycling.

An atomic adsorption spectrometer (PerkinElmer 2380) with graphite oven (PerkinElmer HGA-300 Programmer) was employed for the noble metal detection in liquid solutions. Wavelength was adjusted to 265.9 nm for platinum. The slit size was kept at 0.2 nm (ALT) and data acquisition was 1 s. In each measurement, 25 μL sample of suitable dilution (to fit the linear region of the instrument) was carefully injected into the graphite tube with a fine pipette. An AAS program optimized for platinum determination is shown in Table 2. Standard solutions were prepared from potassium tetrachloroplatinate K_2PtCl_4 (Chempur GmbH Karlsruhe Pt 46.78%). Hydrochloric acid was added to prevent precipitation. The quality of the stock solution with a concentration of 10^{-3} M was frequently examined by UV spectroscopy (between 200 and 700 nm wavelength). It was proven to be stable over month.

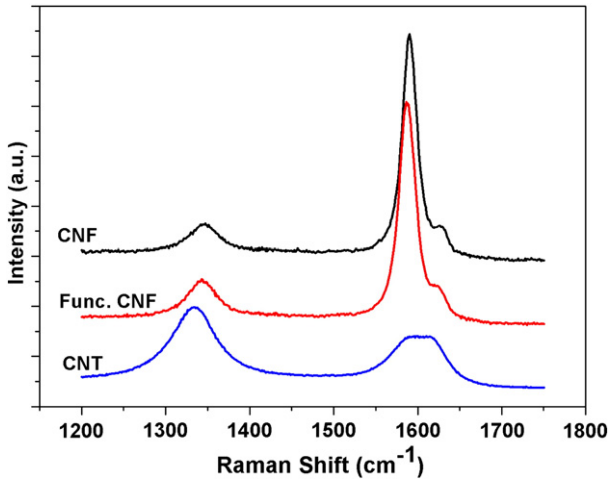

Fig. 2. Raman spectra of CNFs, functionalized-CNFs and CNTs.

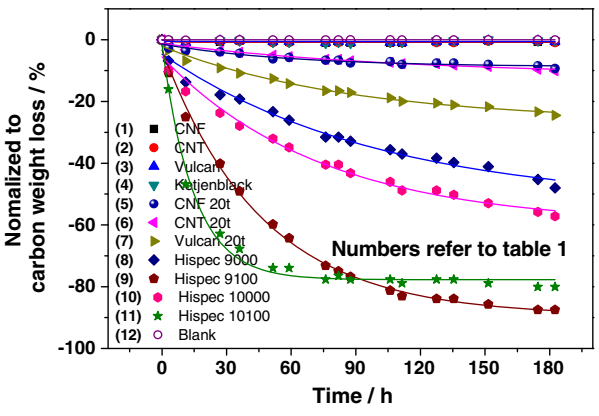

Fig. 3. Carbon and catalyst supported carbon thermal corrosion at 200 °C.

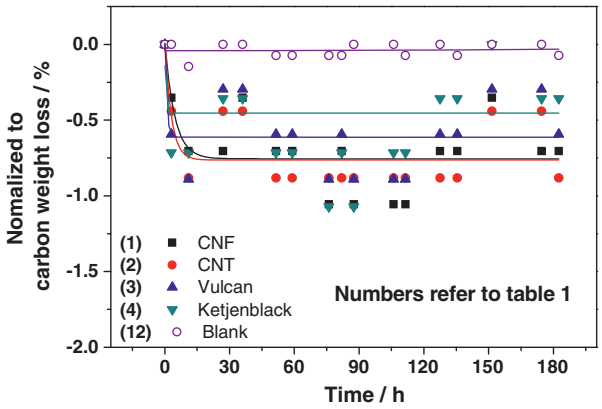

Fig. 4. Carbon thermal corrosion at 200 °C.

2.6. Cyclic voltammetry

MEAs with identical anodes (based on Hispec 9100 catalyst, Pt/C) but different cathode Pt catalyst based on CNF, CNT and Vulcan were prepared with standard procedure, 40 wt.% ionomer content. The cathode was then treated with cyclic voltammetry between 0 and 1.6 V vs. RHE in a single cell with hydrogen purging on the anode and nitrogen purging on the cathode. The electrochemical active surface areas of the cathode catalyst and MEA single cell performance were recorded before and after the treatment, as described later.

2.7. Electrochemical active surface area

The electrochemical active surface area (ESA) of platinum was measured by sweeping potential between 0 and 1.2 V. The evaluation of the platinum surface area is carried out by measuring columbic charge required for monolayer atomic hydrogen adsorption. ESA is calculated with the following equation:

$$ESA = \frac{Q}{[Pt] \times A \times C}$$

ESA : electrochemical surface area $\left[cm^2/mg\right]$
Q : the charge for hydrogen adsorption/desorption, [mC]
$[Pt]$: platinum loading, $\left[mg/cm^2\right]$
A : area, $\left[cm^2\right]$
C : a constant, which is the charge required to oxidize a monolayer of atomic hydrogen on Pt catalyst, in the calculation $C = 0.22\left[mC/cm^2\right]$

2.8. Single cell assessment

Fuel cell testing was performed with a single cell of dimension $1.5 * 1.5\ cm^2$. Pure hydrogen and lab air were used as fuel and oxidant with a flow of 0.2 and 1 mL/s respectively, regulated by a mass flow controller (Brooks). Impedance measurements were performed under a DC load of 0.5 A. The gas was humidified with a power capacity of 1 kW humidifier (FumaTech). The maximum operation temperature was limited to 70 °C. Thermocouples were installed at critical spots for accurate monitoring of the temperature variation during gas transportation. The system was controlled by an electrochemical workstation (IM6, ZAHNER).

3. Results

3.1. Carbon and catalyst characterization

VGCF™ (CNF herein) is a vapor grown highly graphitized carbon nanofibers with an average diameter of 150 nm, whereas VGCF-X™ (CNT herein) is multi-walled carbon nanotubes with an average

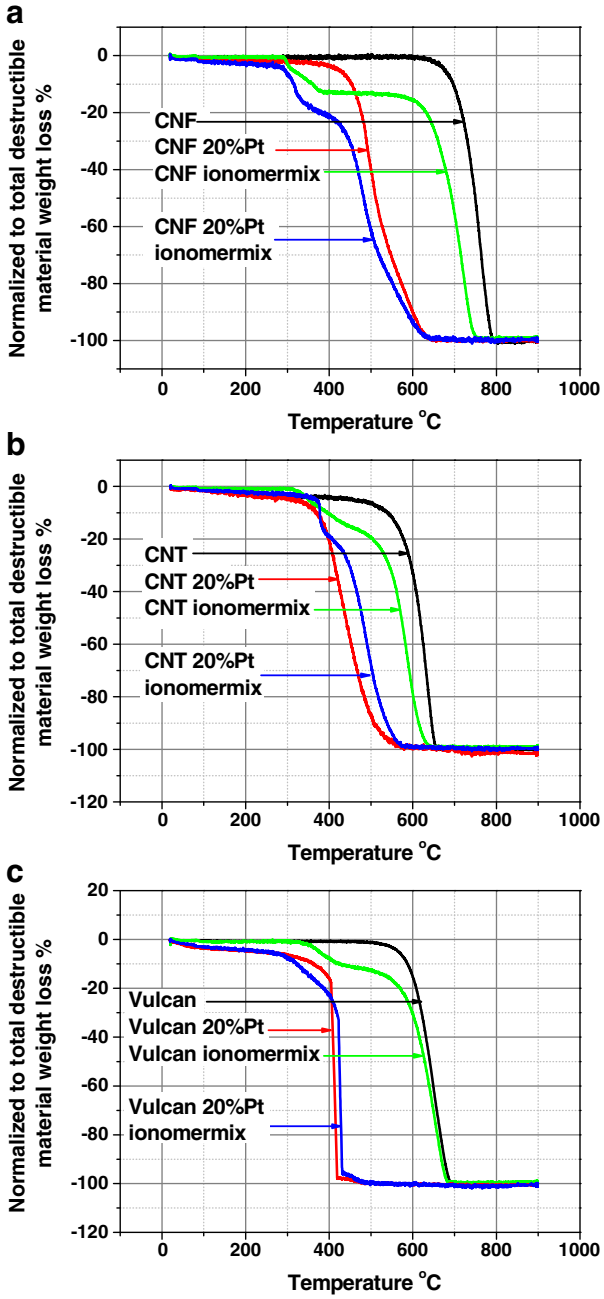

Fig. 5. TG pattern of individual catalyst supports.

diameter of about 15 nm. Their detailed properties can be found in Table 1, and their SEM morphology is shown in Fig. 1(A).

The tube walls of as-received CNFs are rather inert to anchor with metal particles since they have been highly graphitized at elevated temperatures of about 2800 °C. Therefore, CNFs were subjected to different oxidative treatments to promote the deposition of high Pt loadings by introducing binding sites to anchor Pt nano-particles. Different oxidative protocols were carried out in which the nature of the acids (HNO_3, H_2SO_4 or mixture), refluxing time and temperature were varied to optimize the functionalization treatment, in order to achieve a high Pt loading without a significant loss of the stability of the CNFs. The optimized protocol for CNFs was found to be boiling at 120 °C under refluxing conditions for 6 h in a 1:1 mixture of 2 M HNO_3/1 M H_2SO_4, which led to the least structural defects and enabled achieving Pt loadings up to 40 wt.%.

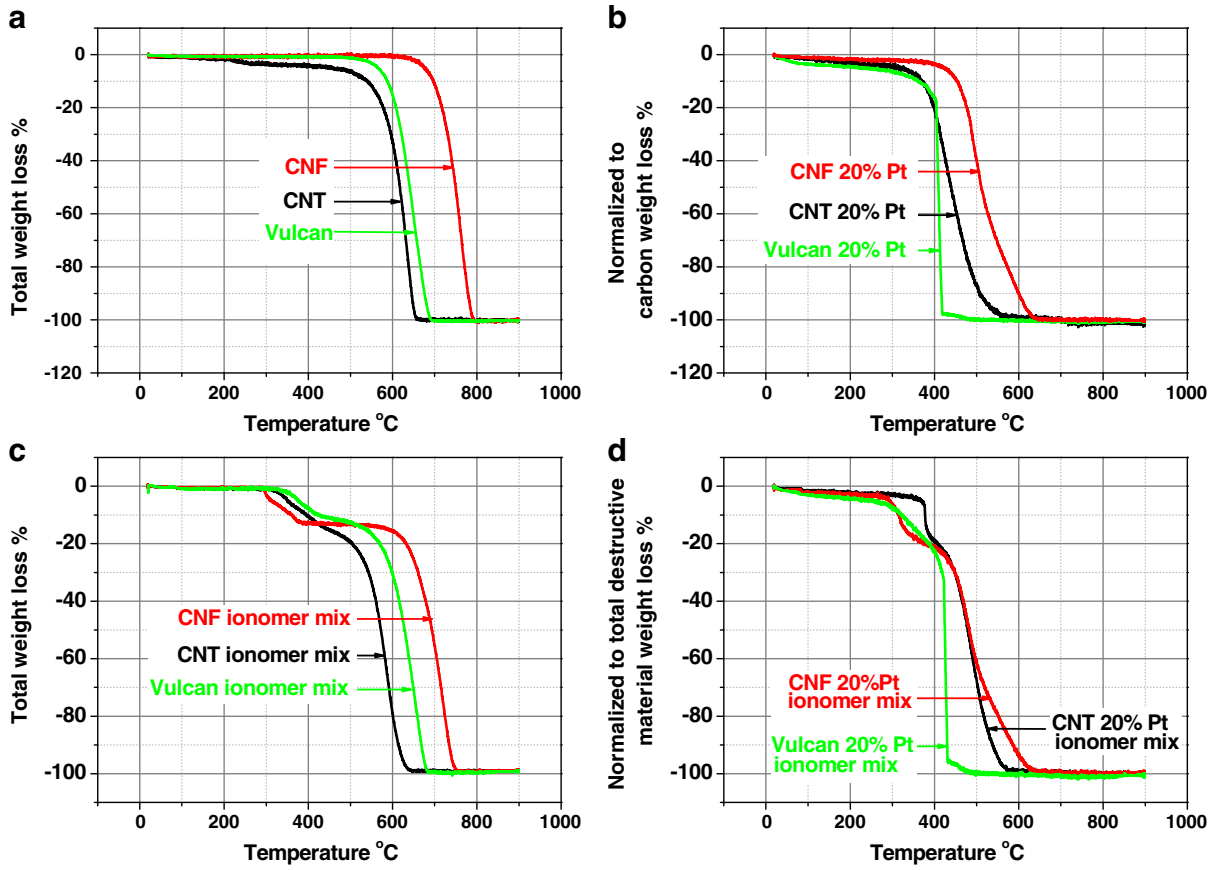

Fig. 6. TG pattern of catalyst support comparison.

Fig. 2 shows the Raman spectra of CNTs, CNFs and functionalized CNFs, illustrating both the characteristic mode for defective graphitic structures (D-band) around 1350 cm^{-1} and the feature of graphitic layers that corresponds to tangentional vibration of the carbon atoms near 1580 cm^{-1} (G-band) [27]. The intensity ratio of D-band to G-band (I_D/I_G) of CNF (0.3) and CNTs (1.45) declares the difference in the morphology of the samples. It has been reported that vacuum annealing of the carbon nanotubes at high temperatures (above 1800 °C) increases the ordering of tube walls, hence the I_D/I_G value decreases and a peak separation of G- and D-band (G-band shoulder peak about 1620 cm^{-1}) appears in the Raman spectra [28]. As discussed above, since CNF walls are highly ordered and resistive to structural damage, the optimized acid treatment introduces minor change in I_D/I_G (0.34) in functionalized CNF sample. Therefore, not only CNT sample with higher I_D/I_G ratio includes more defects in tube walls but also the broad G-band which indicates that the sample may contain nanotubes at different stages of graphitization. Consequently, the further oxidizing treatment of the highly defected surface area CNTs has been prevented to refuse more damage on the tube walls and the target Pt loading on the CNT sample was easily obtained.

Highly dispersed Pt nano-particles of very small and uniform size distribution (2–3 nm) were obtained on both carbon supports, as shown in the TEM images in Fig. 1(B) for Pt/CNF and Pt/CNT respectively.

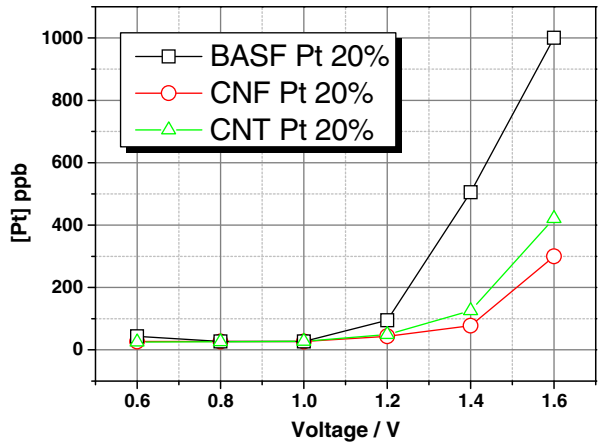

Fig. 7. Platinum dissolution in acidic media at room temperature.

3.2. Thermal stability of carbon

Carbon weight loss at constant temperature is illustrated in Fig. 3. The final value presented in the graph is normalized with respect to the original carbon weight content (based on the condition that carbon is the only destructive material during the experiment, as explained in Section 2.2). The degradation data follow a first order exponential decay $y = A1 * \exp(-x/t1) + y0$. The fitting was performed by Origin®. The corresponding sample information can be found in Table 1. The blank sample is empty aluminum foil. All the values cited in this section refer to the end of the experiment.

CNF & CNT and traditional carbon black demonstrate clear different degradation patterns. Both CNF and CNT based catalysts (#5 & #6, in Fig. 3 and Table 1) showed less than 10% carbon weight loss, while one commercial carbon (#9 and #11, the information of this type of carbon support was unfortunately confidential) showed between 78 and 88% weight loss, and Vulcan based catalysts (#7, #8 and #10) showed between 24 and 55% weight loss depending on the catalyst loading and the catalyst properties: the higher the platinum content, the more vulnerable the carbon is (#7 20% Pt, carbon weight loss ~24%, #8 58% Pt, carbon weight loss ~45%); PtRu type catalyst is seen more efficient

Table 3
Summary for electrode electrochemical stability under cycling voltammetry treatment.

		Loading mg/cm^2	Area cm^2	ESA cm^2/mg	ESA change %	Max power density w/cm^2	Max power density change %
BASF	Fresh	0.518	2.25	779	100	0.393	100
MEA1430-8	After 5k	0.518	2.25	463	59	0.315	80
	After 10k	0.518	2.25	392	50	0.306	78
CNF	Fresh	0.529	2.25	331	100	0.195	100
MEA1431-1	After 5k	0.529	2.25	426	129	0.276	142
	After 10k	0.529	2.25	330	100	0.218	112
CNT	Fresh	0.530	2.25	310	100	0.147	100
MEA1415-2	After 5k	0.530	2.25	328	106	0.176	120
	After 10k	0.530	2.25	248	80	0.156	106

in catalyzing carbon corrosion (the reaction is faster for #10 containing PtRu than #8 only Pt, and faster for #11 containing PtRu than #9 only Pt, based on the same type of carbon support.). For CNF and CNT based catalysts, carbon degrades very similarly. Moreover, both of them are superior to Vulcan based catalysts (BASF and Johnson Matthey).

Fig. 4 is an analysis on only carbon samples (no catalyst involved). It is obvious that they are rather stable over the whole treatment period, less than 1% weight loss was detected. This might also due to re-adsorption of trace amount of water or other gas molecules and organic substances. Within the first 10 h, all samples reached a stable value. Based on the experimental data, no obvious difference was observed for traditional carbon (Vulcan, Ketjenblack) and CNT or CNF type carbons. The carbon corrosion was mainly due to the catalytic oxidation effect from the supported noble metal catalysts.

3.3. Carbon thermal decomposition

The weight changes of destructible material (carbon and Nafion ionomer) in the sample mixture determined by thermogravimetry are summarized in Figs. 5 and 6. The major turning point in the curve is a well recognized combustion of amorphous carbon which came from the destruction of the crystal structure during the experimental process; the minor turning point at lower temperature is due to the decomposition of the organic polymers.

Fig. 5 categorizes the result based on the support carbon type: (a) CNF, (b) CNT and (c) Vulcan. For all the three types of carbons, when they are finely "mixed" with either platinum or Nafion ionomer or both of them, their decomposition temperatures (DT) decrease with different extent. In general, it demonstrates that nanosized platinum is very effective in catalyzing carbon decomposition (illustrated also in Section 3.2); moreover, introducing Nafion ionomer also contributes carbon degradation, as elaborated below.

Fig. 6 categorizes the results based on mixing conditions: (a) only carbons (no mixing), (b) carbons loaded ("mixed") with 20 wt.% Pt, (c) carbons mixed with 20 wt.% ionomer and (d) carbons mixed with both 20 wt.% Pt and 20 wt.% ionomer. Of the pure carbon forms (Fig. 6a), CNF showed highest decomposition temperature (DT) of 749.92 °C, followed by Vulcan 641.73 °C and CNT 615.96 °C. Higher stability of CNF is most likely due to the thermal treatment (at around 2800 °C), which makes it highly graphitic crystalline and inert. The low stability of this type of CNT probably reflects the high defect concentration in the material. The large crystallinity difference is also clearly reflected in Raman spectroscopy (Fig. 2). When nanosized Pt is involved (Fig. 6b), both CNF and CNT showed a higher DT (511.27 °C and 438.69 °C) than Vulcan (411.22 °C). Vulcan was seen more sensitive towards the catalytic oxidation effect from platinum (DT decreases by 25.20% with respect to the pure carbon in the scale of absolute temperature) than CNF (23.33%) and CNT (19.94%). This indicates that platinum nano-particles are more effective in catalyzing carbon black oxidation than catalyzing oxidation of carbon nano-materials. When carbon is mixed with ionomer (Fig. 6c), DT of CNF (693.53 °C) is seen higher than that of Vulcan (628.89 °C), and then follows CNT (572.42 °C). CNF and CNT seem rather sensitive to ionomer (DT decreases by 5.51%, 4.90%) than Vulcan (1.40%), which might be due to a stronger interaction between the CNF/CNT and the Nafion ionomer. A rather low DT of CNT was again due to its defects. When carbon is "mixed" with both Pt and ionomer (Fig. 6d), which is a mere realistic environment in most of the fuel cell recipes, both CNF (482.24 °C) and CNT (478.91 °C) showed better thermal stability than Vulcan (424.07 °C), in which the catalytic oxidation reaction dominates the process.

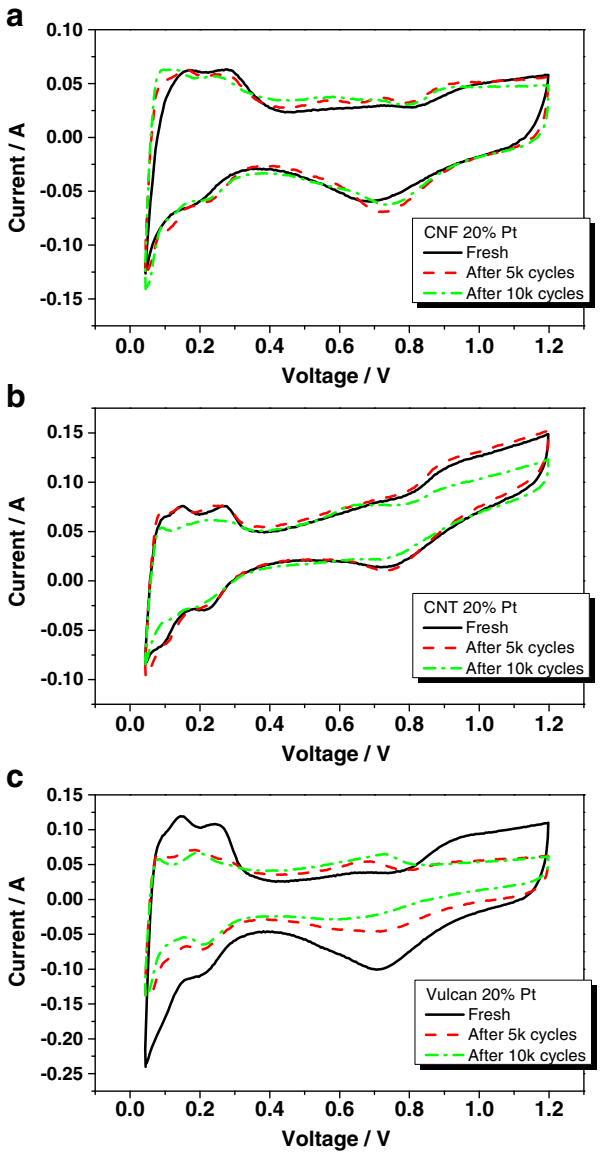

Fig. 8. Examples of ESA determined by hydrogen adsorption.

3.4. Electrochemical stability in acidic aqueous media

Dissolution of platinum on different carbon supports in acidic media at room temperature is shown in Fig. 7. At potentials lower than 1.0 V vs. RHE the three catalysts have very similar dissolution behavior, with platinum concentrations below 30 ppb. This might be due to the similar properties of the finely dispersed noble metal. At higher potentials, platinum dissolution becomes more severe for all the three catalysts; at 1.6 V vs. RHE, CNF, CNT and Vulcan showed Pt concentrations of 300, 421 and 1000 ppb. Comparatively speaking, CNF and CNT supported platinum showed about 3.3 and 2.3 times less dissolution than Vulcan supported catalyst. Platinum dissolution at higher potential has been mainly shown to be due to electrochemical corrosion of carbon support [29]. In addition, based on our experience, at PEM fuel cell working temperature (~80 °C), the platinum dissolution is ten times higher than that at room temperature.

3.4. MEA electrochemical stability under cyclic voltammetry treatment

Electrochemical active surface area (ESA) of the cathode in the MEA and maximum power density measured in the single cell setup before and after the cyclic voltammetry (up to 1.6 V, 5000 cycles and another 10,000 cycles) are summarized in Table 3. Examples of the CV voltammogram are illustrated in Fig. 8. Single cell performance, polarization curves and impedance spectra are shown in Figs. 9 and 10.

Based on the evolution of the electrochemical surface areas (ESA) functioning as number of cycles between 0 and 1.4 V vs. RHE (Fig. 8), both CNF and CNT based cathodes showed better stability than Vulcan based. An increase of ESA was observed in both CNF and CNT based electrodes by 29 and 6% after 5k cycles, which is probably due to an activation process or electrode structure reorganization under performance condition; however Vulcan based electrode showed 41% decrease in ESA after the same treatment. With a further 10k cycles, all the three electrodes showed less ESA than the starting value. This indicates that potential cycling reaching up to 1.4 V vs. RHE is harmful for the electrodes in long term. In the case of CNT based cathode, all CV spectra showed tilted feature (Fig. 8b), which indicates an additional internal resistance around 10.9 Ω. It might be due to low electronic conductivity of the support material, or most likely unoptimized electrode structure. This also leads to inferior performance in single cell, as shown below.

In Fig. 9, showing the I–V curve, CNF and CNT based electrode showed 42 and 20% increase in max power density after 5k cycles; during the same treatment, Vulcan showed 20% decrease, which is also

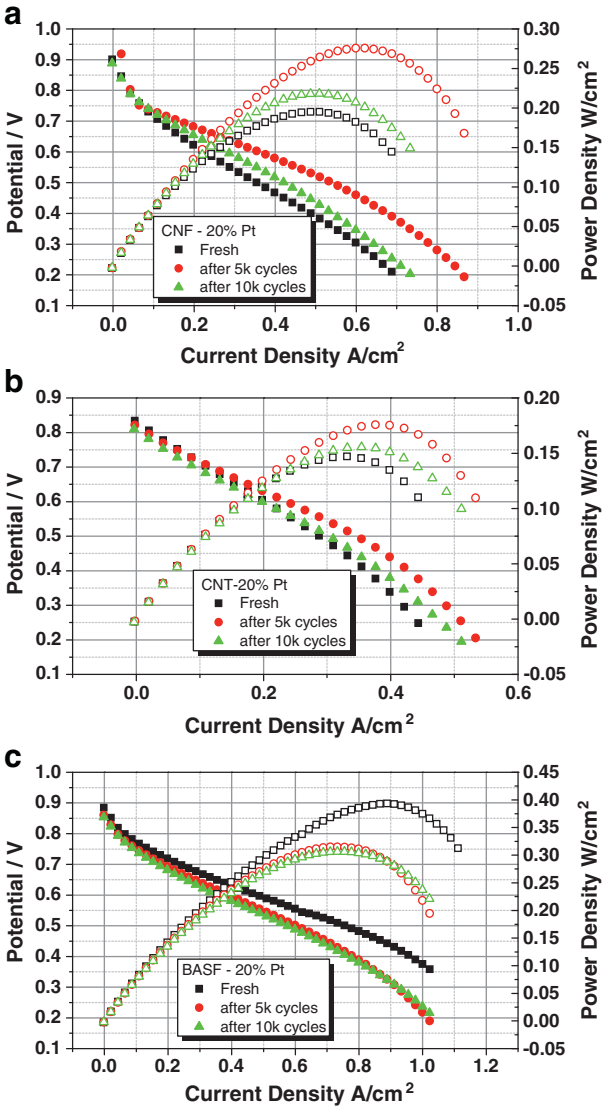

Fig. 9. Single cell performances before and after cyclic voltammetry treatment — polarization curve, H_2 and air are 0.4 and 2 ml/s respectively, 70 °C.

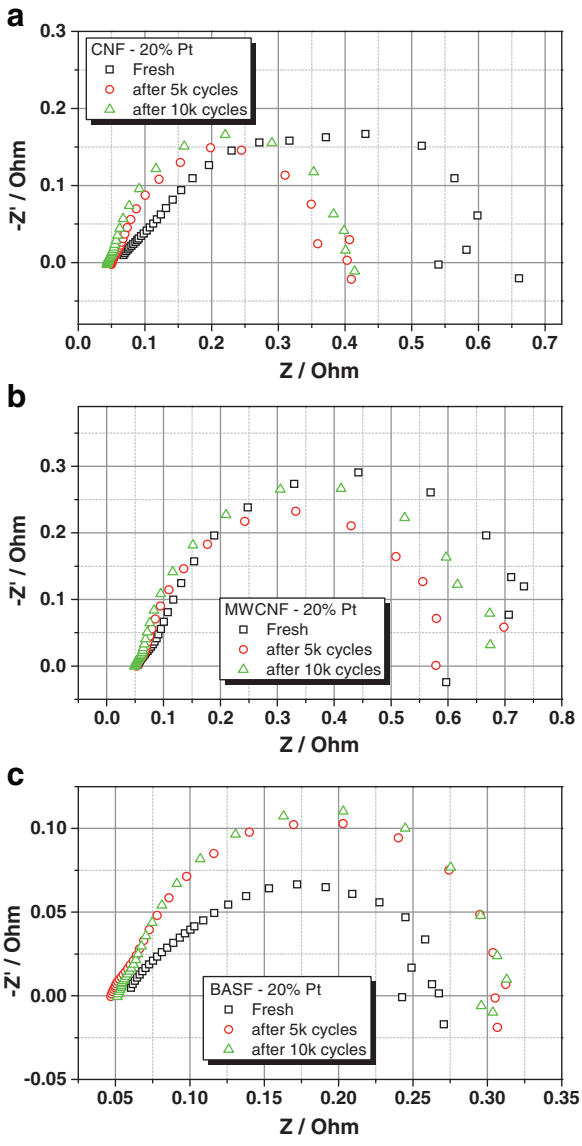

Fig. 10. Single cell performances before and after cyclic voltammetry treatment — impedance, H_2 and air are 0.2 and 1 ml/s respectively, 70 °C.

reflected in the development of the ESA. With further potential cycling, cell performances deteriorate. Similar trends were also observed in impedance spectra in Fig. 10. In all cases, the electrolyte resistance determined from high frequency intercepts decreases, which indicates that improved electrode–electrolyte contact is part of the activation process.

In summary, after cycling to a high voltage (up to 1.6 V), platinum catalysts with carbon nanofiber and carbon nanotube as support showed better stability compared to carbon black (Vulcan) based Pt catalyst. Electrochemical active surface area determined from hydrogen adsorption/desorption can be used to follow the development of single cell performance.

4. Conclusions

Carbon nanofiber (CNF) and carbon nanotube (CNT) supported platinum catalysts were prepared and optimized. The catalysts were evaluated with respect to thermal and electrochemical stabilities with traditional carbon black (Vulcan) based catalyst as reference. From carbon thermal stability, decomposition, electrochemical degradation in acidic aqueous media and cyclic voltage treatments, both carbon nanofiber and carbon nanotube demonstrated better stability than carbon black. High crystalline CNF showed a higher stability than CNT during the entire measurements.

In single cell testing, carbon nanofiber and nanotube based platinum catalyst did not show as good initial power density performance as the equivalent carbon black based ones, but they showed a better durability. CNF & CNT based platinum catalyst PEM fuel cells could therefore provide a more durable and more stable power source. Optimization and activation of the membrane electrode assembly — electrode structure is the key point to gain better cell performance for carbon nanomaterials.

Acknowledgments

The authors give great thanks for the financial support from the Danish PSO—PEM fuel cell durability project (contract no. 2007-1-7156) and Nanouramea project (contract no. 09-064272 by DASTI and contract nos. 124671 and 124769 by the Academy of Finland).

References

[1] A. Nieto-Marquez, R. Romero, A. Romero, J.L. Valverde, J. Mater. Chem. 21 (2011) 1664–1672.
[2] W. Li, H. Ma, X. Li, W. Li, M. Wu, X. Bao, J. Phys. Chem. B 107 (26) (2003) 6292–6299.
[3] M. Okada, Y. Konta, N. Nakagawa, J. Power Sources 185 (2008) 711–716.
[4] G. Yang, G. Gao, G. Zhao, H. Li, Carbon 45 (2007) 3036–3304.
[5] G. Centi, S. Perathoner, Catal. Today 150 (1–2) (2010) 151–162.
[6] F. Darkrim, D. Levesque, J. Phys. Chem. B 104 (29) (2000) 6773–6776.
[7] A.L.M. Reddy, S. Ramaprabhu, Int. J. Hydrogen Energy 32 (17) (2007) 4272–4278.
[8] A.L. Ong, A. Bottino, G. Capannelli, A. Comite, J. Power Sources 183 (1) (2008) 62–68.
[9] S. Zhang, X. Yuan, H. Wang, W. Mérida, H. Zhu, J. Shen, S. Wu, J. Zhang, Int. J. Hydrogen Energy 34 (1) (2009) 388–404.
[10] N. Yousfi-Steiner, P. Mocoteguy, D. Canduss, D. Hissel, J. Power Sources 194 (1) (2009) 130–145.
[11] Y. Shao, G. Yin, Y.J. Gao, Power Sources 171 (2007) 558–566.
[12] X. Yu, S. Ye, J. Power Sources 172 (2007) 145–154.
[13] Y. Zhou, K. Neyerlin, T.S. Olson, S. Pylypenko, J. Bult, H.N. Dinh, T. Gennett, Z. Shao, R. O'Hayre, Energy Environ. Sci. 3 (10) (2010) 1437–1446.
[14] N. Cheng, S. Mu, X. Chen, H. Lv, M. Pan, P.P. Edwardset, Electrochim. Acta 56 (5) (2011) 2154–2159.
[15] S.V. Selvaganesh, G. Selvarani, P. Sridhar, S. Pitchumani, A.K. Shukla, Fuel Cells 11 (3) (2011) 372–384.
[16] L. Li, Y. Xing, J. Power Sources 178 (1) (2008) 75–79.
[17] J.F. Lin, V. Kamavaram, A.M. Kannan, J. Power Sources 195 (2) (2010) 466–470.
[18] H. Wu, D. Wexler, H. Liu, J. Solid State Electrochem. 15 (5) (2011) 1057–1062.
[19] S. Huang, P. Ganesan, B.N. Popov, Appl. Catal., B 102 (1–2) (2011) 71–77.
[20] S. Yin, S. Mu, H. Lv, N. Cheng, M. Pan, Z. Fu, Appl. Catal., B 93 (3–4) (2010) 233–240.
[21] H. Lv, S. Mu, N. Cheng, M. Pan, Appl. Catal., B 100 (1–2) (2010) 190–196.
[22] A. Esmaeilifar, Energy 35 (2010) 3941–3957.
[23] S.L. Knupp, W. Li, O. Paschos, T.M. Murray, J. Snyder, P. Haldar, Carbon 4 (6) (2008) 1276–1284.
[24] W. Li, C. Liang, W. Zhou, J. Qiu, Z. Zhou, G. Sun, Q. Xin, J. Phys. Chem. B 107 (26) (2003) 6292–6299.
[25] Ma S., VDM Verlag, ISBN-10: 363916704X, ISBN-13: 978-3639167047, 2009.
[26] M.C. Tucker, M. Odgaard, P.B. Lund, S. Yde-Andersen, J.O. Thomas, J. Electrochem. Soc. 152 (9) (2005) A1844–A1850.
[27] M.S. Dresselhaus, G. Dresselhaus, R. Saito, A. Jorio, Phys. Rep. 409 (2005) 47–99.
[28] K. Behler, S. Osswald, H. Ye, S. Dimovski, Y. Gogotsi, J. Nanopart. Res. 8 (2006) 615–625.
[29] B. Avasarala, P. Haldar, Electrochim. Acta 55 (16) (2010) 4765–4771.